Stochastic Security Constrained Economic Dispatch for PFR Adequacy under Uncertain Wind Generation

Vivek Prakash[1], Priyanka Kushwaha[2], Kailash Chand Sharma[1], Rohit Bhakar[2] and Harpal Tiwari[2]
[1]Department of Electrical Engineering, School of Automation, Banasthali Vidyapith, India
[2]Department of Electrical Engineering, Malaviya National Institute of Technology Jaipur, India
Email: vivekprakash@banasthali.in

***Abstract*— The stochastic behaviour of modern generation systems poses a formidable challenge for System Operator (SO) to maintain generation-demand balance. This imbalance should be corrected within a short span of time otherwise, system frequency would vary from the nominal value. Large frequency variations due to contingency, like generation outage or loss of load, may cause serious threats to stability and security of the system. This necessitates a wider understanding of the research challenges arising out of large penetration of Renewable Energy Sources (RES) in the grid and requires evolving system technologies and modelling to maintain reliable and secure system operation. This research attempts to develop a mechanism for PFR adequacy with the large integration of uncertain wind generation sources. A novel stochastic security constrained economic dispatch framework is proposed for the assessment of role and value of available and required PFR mapped with frequency security criteria like Rate of Change of Frequency (ROCOF) and Frequency Nadir. This addresses multiple concerns associated with PFR adequacy such as comprehensive modeling of dynamic frequency evolution after contingency, uncertainty characterization, and representation in system operation.**

Keywords- Economic dispatch, primary frequency response, system inertia, stochastic scheduling, uncertainty modelling, wind generation.

I. INTRODUCTION

Rapid installation of wind/PV farms into the grid would displace the conventional generation at a fast rate. Bulk penetration of these generation sources has significant impact on power system security and reliability, due to uncertain and intermittent generation characteristics. Displacement of conventional generation would reduce the system inherent Primary Frequency Response (PFR) capability. Hence, maintaining system PFR adequacy and the prospect of new generation technologies interfacing with the grid create a range of system operational issues for the SO [1],[2].

Generation characteristics of wind are different from those of conventional generation. Wind Speed uncertainties increase the operational risk and affect generator output continuously. Normally, wind generators are installed with frequency relay that isolates after a frequency disturbance. When there is large wind penetration in the grid, a massive wind disconnection could lead to frequency instability. As wind generation share increases, the fluctuations of generated power increases whilst overall system inertia and PFR is reduced. This is due to the fact that wind generators directly can't contribute to the system inertia and PFR capability. Wind generators are having no operation cost and are available throughout the scheduling time horizon [3]. There is a reduction in the frequency nadir and settling frequency because of the lack of inertial response and PFR from wind and the displacement of responsive conventional generation [4].

Frequency at steady state and governor droop parameter is considered in UC formulation for determination of primary reserve adequacy [5]. However, dynamic frequency deviation modelling is not considered. This assessment is reported in security constrained UC (SCUC) and SUC framework [6], [7]. In SCUC formulation, linearized frequency constraints are formulated considering wind generation [8]. However, wind uncertainty impact and its modelling are not considered. Inertia and PFR constraints are included in Modified interval UC model with consideration of wind uncertainty [9]. However, stochastic security constraints are not investigated completely for PFR adequacy. This requires wider understanding of system's frequency stability requirements with large wind penetration.

This paper attempts to develop a stochastic security constrained economic dispatch model for PFR adequacy with the large integration of uncertain wind generation sources. A computational framework is proposed for the assessment of role and value of available and required PFR mapped with frequency security criteria like Rate of Change of Frequency (ROCOF) and Frequency Nadir. This addresses multiple concerns associated with PFR adequacy such as comprehensive modeling of dynamic frequency evolution after contingency, uncertainty characterization, and representation in system operation. Developed models and approaches have been illustrated through realistic case studies. Outcomes of this research would be helpful to understand the PFR challenges with large integration of wind generation.

II. WIND SCENARIO GENARATION-REDUCTION

Power system operations like generation scheduling and dispatch are decision-making problem. Decisions obtained through these operations impact the system security and reliability. Wind power uncertainty makes this problem

This work is supported by the DST grant for UKICERI project, DST/RCUK/JVCCE/2015/02.

more critical [10]. Accurate modeling of involved uncertainties is necessary to solve these decision-making problems. The uncertainty of input parameters could be described by a stochastic process. The stochastic process could be characterized by scenarios. Scenarios are probable outcomes of arbitrary input with corresponding occurrence probability as shown in Fig. 1. Large quantum of scenarios is required for precise modeling of any stochastic process. Computational time required to solve scenario-based approach depends on the quantum of scenarios. Therefore, it is required to reduce original scenarios set, in a manner that reduced set has a lesser number of scenarios, with minimally changed statistical properties.

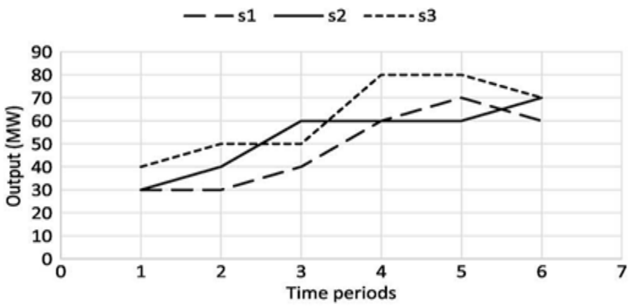

Fig.1. Wind uncertainty modelling illustration through stochastic scenarios.

Statistical ARIMA model is used to model random time series based on a number of historical data, pattern identification, and parameter estimation [11]. This is a hybrid of autoregressive and moving average model. The typical ARIMA (p,d,q) model is expressed as

$$\alpha_p(\beta)(1-\beta)^d \lambda_t = \psi_0 + \psi_q(\beta)\zeta_t \tag{1}$$

where λ_t is the prediction limit of wind & PV power at time interval t, d is the degree of differentiation β is the backshift operator, $\alpha_p(\beta)$ is the AR operator of order p, and $\psi_q(\beta)$ is the MA operator of order q . ζ_t is a random number distributed normally with zero mean and constant variance. This is also known as white noise or error signal. If q is assumed to be zero in ARIMA model, it behaves like an autoregressive (AR) model. Steps for scenario generation and reduction is as follows:

A. Step-Wise Scenario Generation Procedure

In this section, the step-wise procedure for wind power forecast is described.

Step 1: Distribution Fitting: Take historical wind speed power data of any specified site. Fit these data into known probability distribution and estimate the parameters of this distribution.

Step 2: Time Series Analysis: Estimate the order and parameter of time series ARIMA model.

Step 3:Time Counter Initialization: Here 24-time periods are considered for day-ahead scenarios generation. Start with time $t=1$.

Step 4: Evaluate forecasting model.

Step 5: Wind Speed to Power Conversion:

Step 6: Check Time Counter: If desired time period counter, *i.e.* 24 is achieved, go to next step, otherwise update $t=t+1$ and go to step 3.

Step 7: Obtain scenarios.

B. Step-Wise Scenario Reduction Procedure

Large scenario quantum is necessary to precisely model any stochastic process. However, computational burden for solving scenario-based optimization models would increase due to the huge number of scenarios. This necessitates reduction of original scenario set in a manner to obtain reduced number of scenarios without changing the statistical properties [11]. The reduced scenario number is based on the problem type, which is to be optimized, and it must be less than one-fourth of generated scenarios. The basic idea of scenario reduction is to remove scenarios with very low occurrence probability and bundle scenarios that are very close. Accordingly, scenario-reduction algorithms determine a subset of scenarios and calculate probabilities for new scenarios, such that the reduced probability measure is closest to the original probability measure, in terms of a certain probability distance between the two measures [12].

The scenario-reduction algorithm reduces and bundles the scenarios using the Kantorovich Distance (KD) matrix. KD is the probability distance between two different scenario sets that represent the same stochastic process. It is generally used to quantify the closeness of different scenario sets. KD assures that maximum possible scenario are reduced, without violating given tolerance criteria. Probability of all deleted scenarios is assumed to be zero. The new probability of preserved scenarios is equal to sum of its former probability and the probability of deleted scenarios that are closest to it [13].

Step 1: Collect Generated Scenarios: All scenarios generated by using algorithm described in previous section are collected. Assign probabilities of collected scenarios in such a way that sum of probability of all scenarios at any time step must be unity. Probability of each scenario s is $1/N_s$, where N_s is total number of generated scenarios.

Step 2: Compute KD Matrix: Compute the cost matrix for each pair of scenarios and determine the KD matrix by multiplication of scenario probabilities.

Step 3: Scenario Selection: Determine the scenario with lowest KD. The lowest KD is obtained for scenarios with equal magnitude and probability.

Step 4: Scenario Elimination: Select the scenario with lowest KD, and the scenario having KD closest to it. The lowest KD scenario is removed on the basis of its relative closeness to the other scenarios and low occurrence probability. Its probability is added to the probability of nearest identified scenario. This ensures that sum of the occurrence probability of all the remaining scenarios is always unity. This process of scenario reduction gives rise to a new probability matrix with the reduced order.

III. STOCHASTIC SECURITY CONSTRANED ECONOMIC DISPATCH MODEL

The problem objective is to minimize the expected operating cost. The basic scheduling formulation has been modified to incorporate inertia and PFR constraints requirements [14].

A. Objective Function

It considers the cost of each scenario in proportion to its probability. The objective function includes no-load cost, start-up cost and operating cost of all the generators, along with the cost of enabling the governor and lost load cost as shown by Eqn. (2).

$$\min(\Pi_s \sum_{t\in T}\sum_{i\in I} A_i.u_{i,t} + su_{i,t} + LS_t * VOLL + \delta_{i,t}.C_i^{ge} + K_i.g_{i,t,s}) \quad (2)$$

Where, I , T , S , J and are the set of generators, time interval, scenarios and linear segment of cost curve, generator start-up cost and generators without enabled governor respectively, while i , t , s , j are the index of generators, time intervals, scenarios and each generator cost curve, start-up cost, respectively. A_i is no-load cost of generator i ($), $u_{i,t}$ is the generator on/off status variable, $su_{i,t}$ is the variable for start-up cost of generator i during hour t ($), LS_t is denoting the load shedding variable at time interval t (MW), $VOLL$ is the value of loss load ($/MW-h), $\delta_{i,t}$ is the variable for generator governor enabled while c_i^{ge} is the cost of enabling the governor($), π_s is the probability of scenario s , K_i is the generator i cost curve ($/MW) and $g_{i,t,s}$ is the power output of generator i under scenario s during hour t .

B. Generator Operational Constraints

The optimization problem is subject to following operational constraints.

$$y_{i,t} - z_{i,t} = x_{i,t} - x_{t-1,i}, \quad \forall t \in T, i \in I \quad (3)$$

$$y_{i,t} + z_{i,t} \le 1, \quad \forall t \in T, i \in I \quad (4)$$

Constraint (3) determines the generator start-up or shutdown status at the time t , based on its 0/1 status between hours $t-1$ and t . $y_{i,t}$ is the generator start-up status and $z_{i,t}$ is the generator shut down status. Constraint (4) restricts the generator to start up and shut down within the same time interval.

$$\sum_{j\in J} q_{i,t,j} = y_{i,t}, \quad \forall t \in T, i \in I \quad (5)$$

$$su_{i,t} = \sum_{j\in J} SUC_{i,j} \cdot q_{i,t,j}, \quad \forall t \in T, i \in I \quad (6)$$

Constraint (5) & (6) determines the exact points of the start-up curve at which generator has not been in service. The start-up cost of each generator depends on the service hours. Here $q_{i,t,j}$ is the generator start-up cost identification matrix and $SUC_{i,j}$ is the cost of segment j .

$$\underline{G}_i.x_{i,t} \le g_{i,t,n} \le \overline{G}_i.x_{i,t}, \quad \forall t \in T, i \in I, n \in N \quad (1)$$

$$-\underline{R}_i \le g_{i,t,n} - g_{i,t-1,n} \le \overline{R}_i, \quad \forall t \in T, i \in I \quad (2)$$

Power output of individual generators is taken as the sum of the output on each part of its cost curve, as defined by constraint (7). Here, $\overline{G}_i$ and $\underline{G}_i$ denotes maximum and minimum power output of the generator. Constraint (8) sets the up and down ramp limits for each scenario, $\overline{R}_i$ and $\underline{R}_i$ are ramp up and ramp down limit of generator.

C. Transmission Constraints

$$\sum_{i\in n} g_{i,t,s} + \sum_{w\in n}(W_{w,t,s} - c_{w,t,s}) - \sum_{\{n,m\}\in L} B_{sm}(\theta_{n,t,s}) = D_{t,n}, \forall t \in T, s \in S, n \in N \quad (9)$$

$$0 \le c_{w,t,s} \le W_{w,t,s}, \forall t \in T, w \in W, s \in S \quad (10)$$

$$-L_{nm} \le B_{nm}(\theta_{m,t,s} - \theta_{n,t,s}) \le L_{nm}, \quad \forall t \in T, \{n,m\} \in L, s \in S \quad (11)$$

$$-\pi \le \theta_{n,t,s} \le \pi, \forall t \in T, n \in N \setminus n_{ref}, s \in S \quad (12)$$

$$\theta_{n_{ref},t} = 0, \forall t \in T \quad (13)$$

Where,

B_{nm}	Line admittance between n and m (S).
$D_{t,\mathrm{n}}$	Bus n load in time interval t (MW).
$\theta_{\mathrm{n},t,\mathrm{s}}$	Voltage angle at bus n , time interval t , scenario s (radian).
$c_{w,t,\mathrm{s}}$	Wind farm w power curtailment, time interval t , scenario s , (MW).
L_{nm}	Lines n and m capacity (MW).

Power balance equation at each node is given by Eqn. (9). Eqn. (10) defines limits of wind power loss at each wind generator. If the line flow limits mentioned in Eqn. (11) could not be a specific value of wind power available at the wind farm w , the wind power is curtailed by $c_{t,w,s}$. Voltage angle limits are set by Eqn. (12), which is set to 0 for reference bus in (13).

D. PFR and System Inertia Constraints

PFR constraints aims to control the initial deviation of frequency within prescribed limit, following a maximum infeed loss. Constraint (14) ensures that enough inertial response should be available so that the maximum RoCoF does not trigger protective relays like UFLS relay or cause instability. Here H_i is the inertia constant of generator i , H^{load} is equivalent load inertia (s), H^{req} is the required inertia (s). Constraint (15) ensures PFR adequacy, $Pf_{i,t}$ is the variable for total PFR availability (MW), P^C is the constant for PFR capacity requirement (MW), ε is the load damping rate (1/Hz) and $\Delta f^{\max}$ is the maximum frequency deviation (Hz). Constraint (16) generates the equivalent droop curve R^{dre}, represented as Hz/MW. Eqn. (17) ensure that adequate headroom is available with enabling of governor for providing PFR and maintaining the droop curve relationship. Constraint (18) requires the generator to be online when its governor is enabled. Constraint (19) disables the generators by assigning u equal to 0, which are working in the mode that couldn't provide PFR, while constraint (20) sets δ equal to 0 for the generators having large governor dead-band.

$$\sum_{i\in I}\left\{u_{i,t}*H_i*\overline{G}\right\}+H^{load}*D_{t,n}\geq H^{req}-R_t^{ins}\forall t\in T \quad (14)$$

$$\sum_{i\in I}Pf_{i,t}\geq P^{C}-\varepsilon*P_{t,b}^{d}*\frac{\Delta f^{\max}}{f_0}-R_{t,}^{ins},\quad \forall t\in T \quad (15)$$

$$R_i^{dre}=\frac{R_i^{drc}*f_0}{\overline{G}_i},\qquad \forall i\in I \quad (16)$$

$$Pf_{i,t}\leq\frac{\delta_{i,t}}{R_i^{dre}}(\Delta f^{\max}-G_i^{db}),\quad \forall i\in I,\forall t\in T \quad (17)$$

$$Pf_{i,t}\geq\frac{\Upsilon_{i,t}}{R_i^{dre}}(\Delta f^{\max}-G_i^{db})-\overline{G}_i(1-\delta_{i,t}),\forall i\in I,\forall t\in T \quad (18)$$

$$\delta_{i,t}\leq u_{i,t}\forall i\in I,\quad \forall t\in T \quad (19)$$

$$\delta_{i,t}=0\quad \forall i\in G^{ng},\quad \forall t\in T \quad (20)$$

Eqn. (21) and (22) checks the requirements of PFR and ensures that adequate PFR is available at nadir time, t^{nadir} and intermediate steady-state time, t^{ss}.

$$\sum_{i\in I}Pf_{i,t}\geq P_{i,t}^{ss}-P^{Css}\qquad \forall t\in T \quad (21)$$

$$\sum_{i\in I}P_{i,t}^{nadir}\geq P_{i,t}^{reqnadir}-P^{Cnadir}\qquad \forall t\in T \quad (22)$$

IV. WIND POWER SCENARIOS

Table 1 gives the reduced wind power scenario with corresponding probabilities and KDs for eleventh hour. This table shows that Scenario 3 has the lowest KD and would be selected for elimination in the next iteration. Scenario 9 is closest to the selected scenario. The new probability of Scenario 8 would be the sum of its previous probability and probability of Scenario 3. Wind speed historical time series data for the duration 01.01.2016 to 31.12.2016 is used, online available from Illinois Institute of Rural Affair, USA [15]. Wind power uncertainty is modelled in proposed model by considering 1000 wind power scenario generations. After scenario generation, backward reduction algorithm is utilized to obtain 10 representative scenarios. It is observed that both generated and reduced scenarios vary around their mean value, with 95% confidence interval. Reduced wind power scenarios are used in proposed stochastic model for modeling wind power uncertainty.

TABLE I REDUCED WIND POWER SCENARIOS, PROBABILITIES AND KD OF ELEVENTH HOUR

Scenario Index	Wind Power (kW)	Probability	KD
1	1273	0.001	133.665
2	1273	0.001	133.665
3	**77**	**0.001**	**8.085**
4	353	0.001	37.065
5	77	0.001	8.085
6	1273	0.415	133.665
7	353	0.213	37.065
8	886	0.001	93.03
9	**77**	**0.281**	**8.085**
10	886	0.085	93.03

V. CASE STUDY

Test system used to implement the stochastic security constrained economic dispatch model is considered from [16]. In the test system, there are 24 buses, including 17 load buses and 32 generators. The generating units include eleven oil/steam turbine units, nine coal/steam turbine units, six hydro turbine units, four oil/combustion units and two nuclear units. The total installed capacity of generators in one area is 3405 MW with peak load 2850 MW. The data is modified to include 1000 MW generation from wind plant. The penetration level is varied in 10 to 30% range. Nominal frequency (=50 Hz), governor droop (= 5%), frequency dead band (=15 mHz), load damping rate (=1%/Hz), RoCoF of 0.5 Hz/s and delivery time (=10 s) are chosen according to National Grid standards [17]. The largest generators in the system are two nuclear units of 400 MW, and infeed loss of one of the unit is considered. PFR capacity of system should limit frequency above minimum value of 49.2 Hz. The maximum requirement is assumed to be 30% of the total responsive capacity and for all the governors should at least be greater than 100 mHz. is assumed to be 10000 $/MW-h.

A. PFR Analysis

This section details the performance of PFR parameter, considering largest generation outage. The response provided by each unit is shown in Fig. 1.

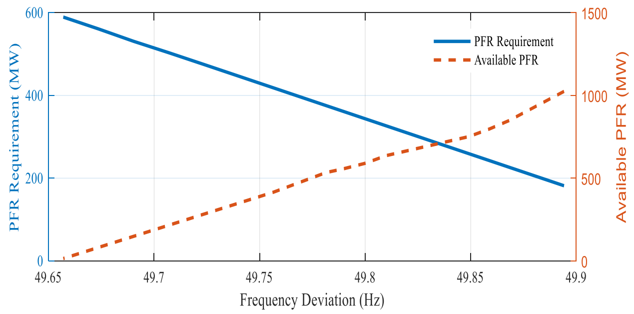

Fig. 2. PFR availability and requirement with frequency deviation.

As the system inertia and PFR capacity reduces frequency deviation increases and frequency reaches the nadir value in lesser nadir time. Hence additional PFR is required to maintain the frequency to the prescribed network limits.

B. Cost Performance

With increasing wind penetration, operation cost reduces. Increasing wind penetration reduces the average number of conventional units committed online per hour.

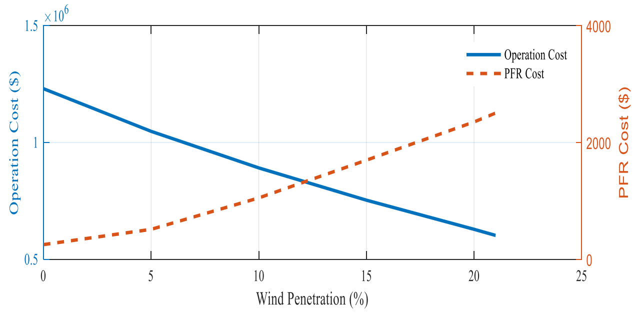

Fig. 3. Operation cost and PFR cost with varying wind penetration.

It could be observed from Fig. 3, there is marginal increment in PFR cost. PFR constraints add only about 0.3% to total operation cost. This marginal increment in PFR cost is because of system's inertia and PFR adequacy. Synchronous inertial cost is considered zero for scheduling horizon, as system has sufficient inertial response and PFR. Fig. 4 shows the variation of operation cost with change in ROCOF and frequency deviation. It could be observed that operation cost is increasing with the fast ROCOF. Similarly increase in frequency deviation value results in increased operation cost.

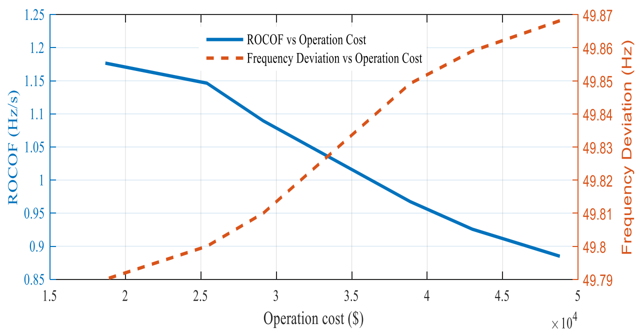

Fig. 4. Operation cost with variation in ROCOF and frequency deviation.

VI. Conclusion

This paper presents a computational framework to assess PFR adequacy in stochastic security constrained economic dispatch model. In this work ROCOF and frequency nadir are control variables to assess systems PFR adequacy under uncertain wind generation. ARIMA model is used for the scenario generation of wind power time series, backward reduction algorithm is used to reduce these scenarios to obtain the representative scenarios required in SUC model for the wind power uncertainty modelling. Case studies are performed to assess the PFR availability and requirement with analysis of cost performance. Numerical results show that with increased wind uncertainty in the system PFR requirement would be higher and this would incur higher cost to maintain system frequency stability. Proposed model could be enhanced by incorporation of PFR pricing and real time procurement of PFR with variation in system inertia condition.

References

[1] S. Sharma, S. Huang, and N. Sarma, "System inertial frequency response estimation and impact of renewable resources in ERCOT interconnection*," IEEE PES GM*, San Diego, July 2011.

[2] V. Prakash, R. Bhakar, H. Tiwari, H. Pain, Y. Bian, and F. Li, "Primary frequency response in future low carbon scenario: Opportunities & challenges," *International Conference on Recent Advances and Innovations in Engineering (ICRAIE)*, Jaipur, Dec. 2016.

[3] V. Prakash, K. C. Sharma, R. Bhakar, H. P. Tiwari, S. Sreekumar, S. Chawda, and F. Teotia, "Primary frequency response with stochastic scheduling under uncertain photovoltaic generation," *IEEE PES GM*, July 2017.

[4] M. Dreidy, H. Mokhlis, S. Mekhilef, "Inertia response and frequency control techniques for renewable energy sources: A review," *Renew. Sust. Ener. Reviews,* pp. 144-155, Nov. 2016.

[5] J. F. Restrepo and F. Galiana, "Unit commitment with primary frequency regulation constraints," IEEE Trans. Power Syst., vol. 20, no. 4, pp. 1588–1596, Nov. 2005.

[6] H. Ahmadi and H. Ghasemi, "Security-constrained unit commitment with linearized system frequency limit constraints," *IEEE Trans. Power Syst*., vol. 29, no. 4, pp. 1536–1545, July 2014.

[7] F. Teng, V. Trovato, and G. Strbac, "Stochastic scheduling with inertia-dependent fast frequency response requirements," *IEEE Trans. Power Syst*., vol. 31, no. 2, pp. 1557–1566, Mar. 2016.

[8] R. Doherty et al., "An assessment of the impact of wind generation on system frequency control," IEEE Trans. Power Syst., vol. 25, no. 1, pp. 452–60, Jan. 2010.

[9] V. Prakash, K. C. Sharma, R. Bhakar, H. P. Tiwari and F. Li, "Frequency response constrained modified Interval Scheduling Under Wind Uncertainty," *IEEE Trans. Sust. Energy*, vol. 9, no. 1, pp. 302-310, Jan. 2018.

[10] V. Prakash, R. Bhakar, and H. P. Tiwari "Stochastic scheduling of primary frequency response for uncertain low carbon power system" *1st Intl. Conf. Large-Scale Grid Integ. In India*, Delhi, Sept. 2017.

[11] K. C. Sharma, P. Jain, and R. Bhakar, "Wind power scenario generation and reduction in stochastic programming framework," Elect. Power Compo. Syst., vol. 41, no. 3, pp. 271–285, Jan. 2013.

[12] H. Pandzic, Y. Dvorkin, T. Qiu, Y. Wang, and D. S. Kirschen, "Toward cost-efficient and reliable unit commitment under uncertainty," IEEE Trans. Power Syst., vol. 31, no. 2, pp. 970–982, Mar. 2016.

[13] D. C. Montgomery, C. L. Jennings, and M. Kulahci, Introduction to Time Series Analysis and Forecasting, New York, NY, USA: Wiley, 2008.

[14] V. Prakash, K. C. Sharma, R. Bhakar, and H. P. Tiwari, "Modified interval-based generator scheduling for PFR adequacy under uncertain PV generation," *IET Gen. Trans. & Distr*., doi: 10.1049/iet-gtd.2018.6391, June 2019.

[15] "Wind speed data", [Online]. Available: http: https://www.renewables.ninja/.

[16] Reliability Test System Task Force, "The IEEE reliability test system—1996," IEEE Trans. Power Syst., vol. 14, no. 3, pp. 1010–1020, Aug. 1999.

[17] National Grid, Security and Quality of Supply Standards [Online]. Available:http://www2.nationalgrid.com/UK/Industry-information/ Electricity-codes/System-Security-and-Quality-of-Supply-Standards/.